

Facile synthesis and Electrochemical Properties of Active Carbon/MnO₂ composites

Qian ZHANG^a, Wang NI^b, Wen-Cheng HU^c

State Key Laboratory of Electronic Thin Films and Integrated Devices, University of Electronic Science & Technology of China, Chengdu 610054, P. R. China

^azhangqiangba@163.com, ^bniwang1226@gmail.com, ^chuwc@uestc.edu.cn

*huwc@uestc.edu.cn

Keywords: AC/MnO₂ composite materials, Specific capacitance, Supercapacitor

Abstract. MnO₂ is directly deposited on active carbon (AC) to synthesize AC/MnO₂ composite to improve the capacitance of electrode material. AC/MnO₂ composites are characterized by X-ray diffraction (XRD), scanning electron microscopy (SEM) and N₂ adsorption-desorption, and the electrochemical properties are evaluated by cyclic voltammetry (CV) and galvanostatic charge/discharge (GCD) test in 1M Na₂SO₄ aqueous solution. The results suggest that the AC/MnO₂ composites show a double layer capacitive behavior in the potential window of -1~0 V. The specific capacitance of AC/MnO₂ (250 F g⁻¹ at current densities of 2A/g⁻¹) is notably higher than that of AC (200 F g⁻¹ at current densities of 2A/g⁻¹).

Introduction

The development of energy storage devices has attracted a great attention due to the depletion of fossil fuels and environmental pollution[1-3]. Supercapacitor has the advantages of high power density, rapid charging/discharging, longer service time and good temperature characteristics [4-6]. It is a new kind of efficient and practical energy storage device.

The energy density of a supercapacitor mainly depends on the nature of electrode materials. Several materials which have been made in previous investigations are capable of delivering high energy density. Carbon[7], transition metal oxides [8-10] and conducting polymer [11, 12] based materials have been traditionally used. Carbon materials due to their good conductivity, high surface area and favorable mechanical integrity, have been proved to be good candidates for electrode materials of supercapacitor, but low capacitance and energy densities limit further development.

In order to obtain excellent capacitance and high energy densities, transition metal oxides are employed to modify the carbon materials, such as MnO₂[13, 14], and Co₃O₄[15, 16]. Manganese dioxide is a material with the advantage of high specific capacitance, and widely used as an electroactive material with low cost of raw materials. However, the poor electronic conductivity of MnO₂ limits the facilitated ion/electron transport, leading a poor capacitive performance.

In the present work, the AC/MnO₂ composite is prepared through a reduction reaction between potassium permanganate and AC. The prepared AC/MnO₂ composite displays a high specific capacitance in 1.0 M Na₂SO₄ electrolyte and an excellent cycling stability with 88.5% capacitance retention after 1000 cycles.

Experimental

Sample Preparation

All chemicals were of analytical grade and were used without further purification. 80 mg of KMnO₄ was dissolved in 60 mL deionized water and 200 mg of AC was added to the above solution under magnetic stirring at 80°C for 6h. After cooling to room temperature, the product was centrifuged and washed with ethanol for three times, and then dried at 80 °C in vacuum oven for 12 h.

Characterization

The surface characterization of the materials was evaluated by the N_2 adsorption/desorption isotherms based on Brunauer–Emmett–Teller (BET) theory, and was determined using a high-speed surface area and pore size analyzers (NOVA 2000e, Quantachrome Instrument, US). The surface morphologies and nanostructures of the AC/MnO₂ were observed using an X-ray diffractometer (D-Max-c type A, RigakuCo. Japan) with a Ni-filtered Cu Ka radiation and a 0.15406 nm wavelength operated at 40 kV and 40 mA. Data were obtained from $2\theta = 20^\circ$ to 90° at a scan rate of 4 per step.

Electrochemical Measurements

To prepare the AC/MnO₂ hybrid coating electrode sheets, the as-prepared powders were mixed with carbon black and styrene-butadiene rubber (SBR, 20 mg mL⁻¹) at a mass fraction of 8:1:1. The viscous slurry was laminated on a 1 mm-thick nickel foam and dried in a vacuum oven at 80°C for 12 h.

Three electrode data were collected using a MetrohmAutolab B.V. electrochemical workstation (PGSTAT302N, Netherlands) with a three-electrode system. All tests were performed in a 1 M Na₂SO₄ aqueous solution at room temperature and normal pressure. A platinum wire, the active materials and a saturated calomel electrode (SCE) were used as counter, working and reference electrodes. GCD tests were performed in the three-electrode system by using a CT2001A rapid sampling battery testing system (LAND, China) at room temperature.

Results and Discussion

Fig. 1 Shows the XRD patterns of the AC and AC/MnO₂ composite. The AC possesses two broad peaks at 26° and 43° indicating the microcrystalline graphitic character. The XRD pattern of AC/MnO₂ composite with weak diffraction peaks located at 12.40° , 18.10° , 37.20° , 43.97° , 65.11° and 78.95° suggesting a poor crystallinity of MnO₂ in the composite, which is favorable for the supercapacitor.

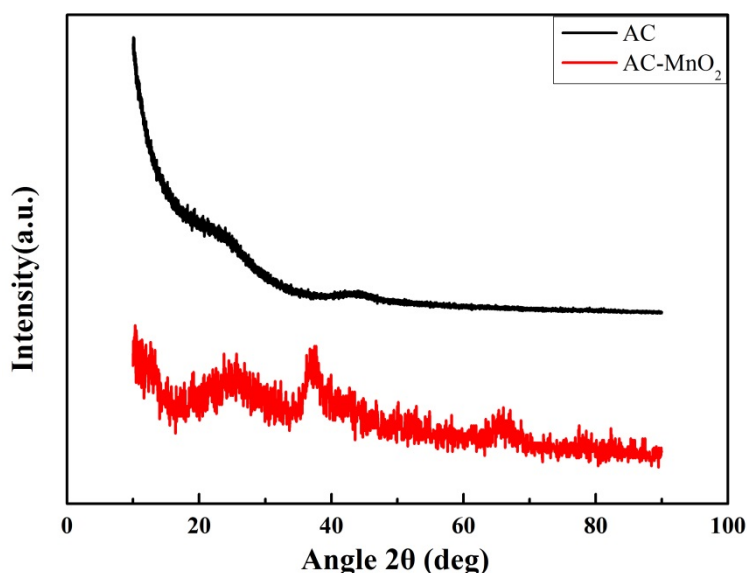


Fig. 1 (A) XRD pattern of AC; (B) XRD pattern of AC/MnO₂

Fig. 2 shows the morphologies of the AC and AC/MnO₂ composite. As shown in Fig. 2(A), the AC is composed of smooth particle with prominent edges and corners. It can be found in Fig. 2(B) that clubbed nanoparticles are deposited on the surface of AC which results in the improvement of capacitance [17].

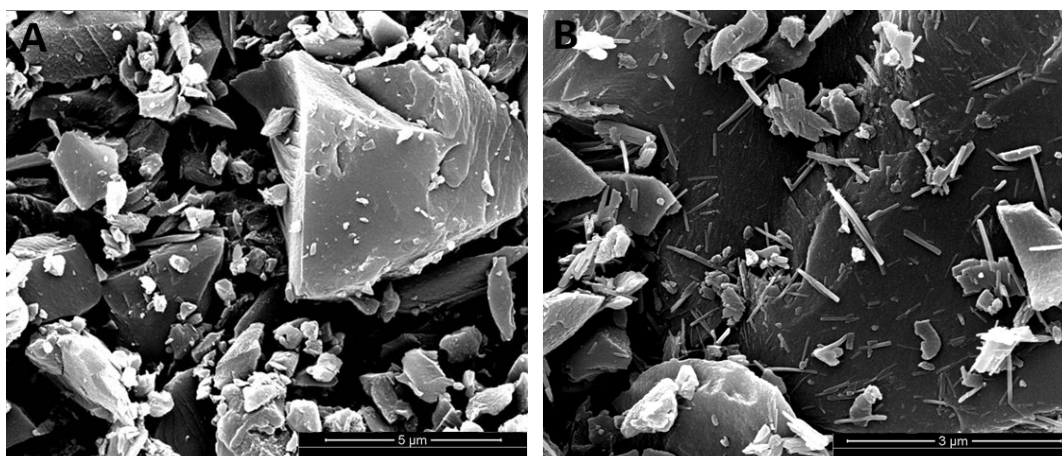


Fig. 2 SEM images of (A) AC and (B) AC/MnO₂

The pore structure property and specific surface area of the AC are measured from the N₂ adsorption–desorption measurements at 77 K. As shown in Fig.3 (A), the AC sample exhibits a type-I isotherm well-defined plateaus, suggesting a microporous nature of the AC. The AC shows a high BET specific surface area of 1657.2m²g⁻¹ and the pore volume is 0.86cm³g⁻¹. In Fig. 3(B), after MnO₂ nanoparticles deposited on the surface of AC, the AC/MnO₂ composite shows a smaller surface area (1087.7m²g⁻¹) and pore volume (0.60 cm³g⁻¹).

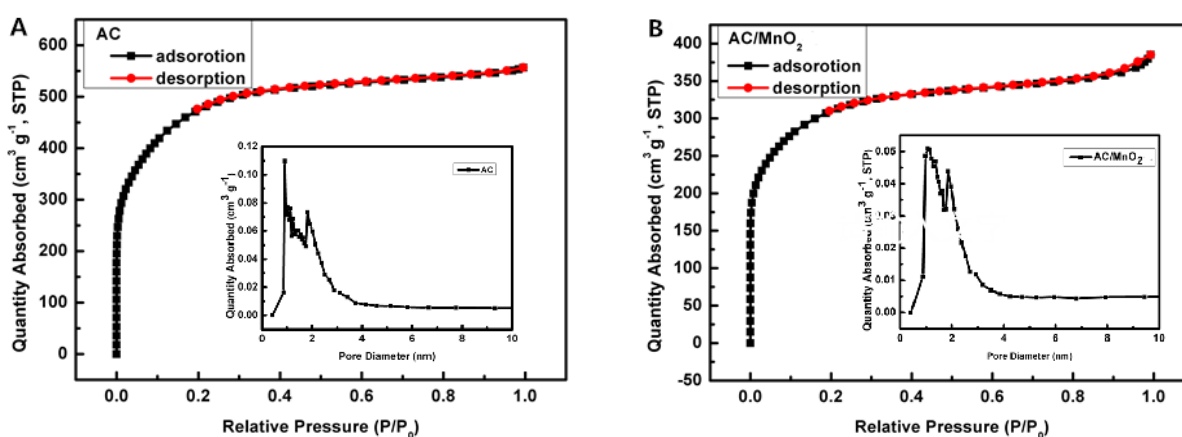


Fig.3. N₂ adsorption–desorption isotherms of (A) AC and (B)AC/MnO₂

CV measurements are performed to evaluate the electrochemical properties of the AC and AC/MnO₂ composite in a 1M Na₂SO₄ electrolyte using a three electrode system. Fig. 4(A) shows the CV curves of AC from -1V to 0V at scan rates of 1–100 mV/s, which exhibit a quasi-rectangular shape, indicating that the main contribution to the capacitance is the charge and discharge of the electrical double layer. In Fig. 4(B), the CV curves of the AC/MnO₂ are close to a rectangle without a redox peak in the potential range of -1-0 V. According to the previous reports [18], the charge storage mechanism of AC/MnO₂ in Na₂SO₄ electrolytes could be described as the eq (1)



The capacitance values of AC and AC/MnO₂ composite obtained from GCD experiments. As shown in Fig. 4 (C), the charge and discharge curves have a triangular shape which corresponds to a capacitive behavior, which indicates that the electrode materials retain good electrochemical properties and quickly undergo ion exchange in the charge–discharge process. In order to evaluate the durability of AC/MnO₂, the charge–discharge cycling test is performed at a current density of 2 A/g⁻¹, which is shown in Fig. 4(D). Apparently, the AC/MnO₂ composite presents a good electrochemical stability with 88.5% capacitance retention after 1000 cycles.

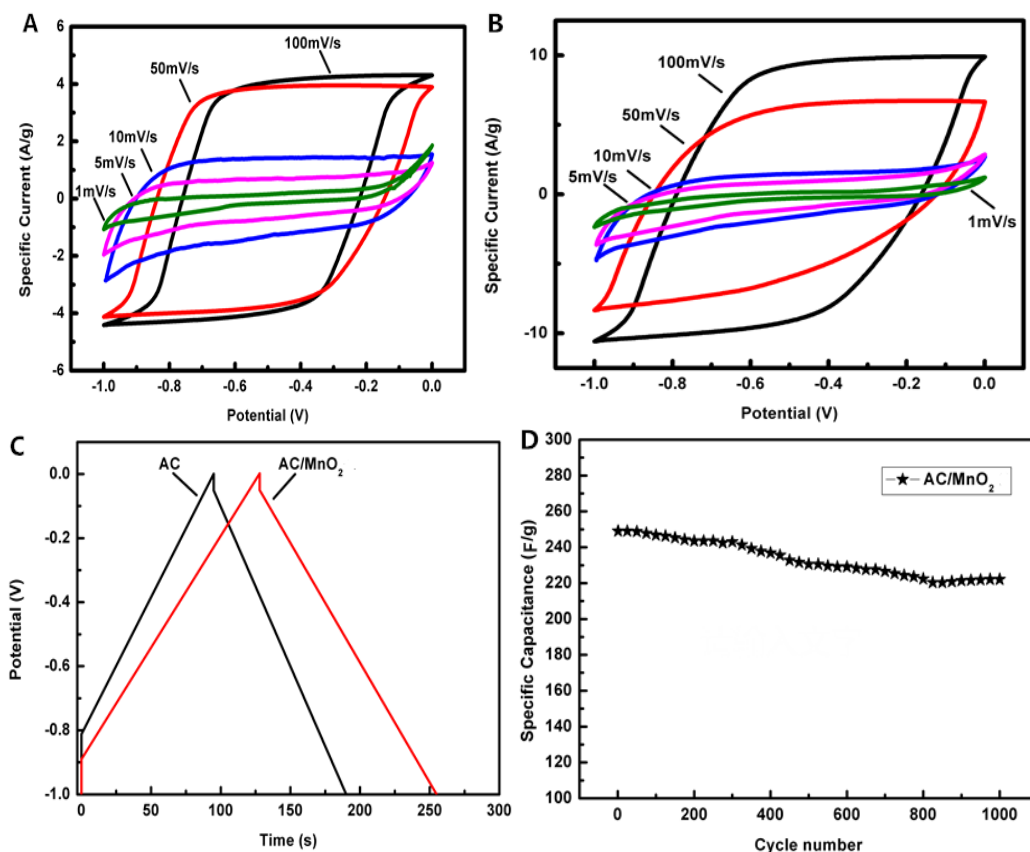


Fig.4. Electrochemical performances of composites in a three-electrode system: (A) CV curves of AC at different scan rates; (B) CV curves of AC/MnO₂ at different scan rates; (C) GCD profiles of AC and AC/MnO₂ at a charge discharge current density of 2 A g⁻¹; (D) The cycling performance of AC/MnO₂ exhibits capacitance retention after 1000 cycles at a charge discharge current density of 2 A g⁻¹.

Conclusions

We suggest a facile and inexpensive process to prepare AC/MnO₂ composite for electrode material of supercapacitor. The AC/MnO₂ composite shows an excellent electrochemical performance due to the high specific surface area and composite structure. The capacitance of the AC based materials is highly improved after the AC coated with MnO₂. The CV curves show a quasi-rectangular shape in the potential range of -1–0 V. The charge–discharge cycle test delivers a triangular shape and a high capacitance of 250 F g⁻¹ at a current density of 2 A/g⁻¹, which is increase about 25% comparing with the pure AC. It also possesses a good electrochemical stability with 88.5% capacitance retention after 1000 cycles..

References

- [1] Chen, W., C. Xia, and H.N. Alshareef, One-step electrodeposited nickel cobalt sulfide nanosheet arrays for high-performance asymmetric supercapacitors. *ACS nano*, 2014. 8(9): p. 9531-9541.
- [2] Wang, Z. and C.-J. Liu, Preparation and application of iron oxide/graphene based composites for electrochemical energy storage and energy conversion devices: Current status and perspective. *Nano Energy*, 2015. 11: p. 277-293.
- [3] Zhu, J., Z. Xu, and B. Lu, Ultrafine Au nanoparticles decorated NiCo₂O₄ nanotubes as anode material for high-performance supercapacitor and lithium-ion battery applications. *Nano Energy*, 2014. 7: p. 114-123.

- [4] Xu, W., et al., Facile hydrothermal synthesis of tubular kapok fiber/MnO₂ composites and application in supercapacitors. *RSC Advances*, 2015. 5(79): p. 64065-64075.
- [5] Yuan, F.-W. and H.-Y. Tuan, Scalable solution-grown high-germanium-nanoparticle-loading graphene nanocomposites as high-performance lithium-ion battery electrodes: an example of a graphene-based platform toward practical full-cell applications. *Chemistry of Materials*, 2014. 26(6): p. 2172-2179.
- [6] Zhu, J., et al., Graphene double protection strategy to improve the SnO₂ electrode performance anodes for lithium-ion batteries. *Nano Energy*, 2014. 3: p. 80-87.
- [7] Jariwala, D., et al., Carbon nanomaterials for electronics, optoelectronics, photovoltaics, and sensing. *Chemical Society Reviews*, 2013. 42(7): p. 2824-2860.
- [8] Chen, P.-C., et al., Preparation and Characterization of Flexible Asymmetric Supercapacitors Based on Transition-Metal-Oxide Nanowire/Single-Walled Carbon Nanotube Hybrid Thin-Film Electrodes. *ACS nano*, 2010. 4(8): p. 4403-4411.
- [9] Flahaut, E., et al., Carbon nanotube–metal–oxide nanocomposites: microstructure, electrical conductivity and mechanical properties. *Acta Materialia*, 2000. 48(14): p. 3803-3812.
- [10] Zhi, L., et al., Precursor-Controlled Formation of Novel Carbon/Metal and Carbon/Metal Oxide Nanocomposites. *Advanced Materials*, 2008. 20(9): p. 1727-1731.
- [11] Kan, X., et al., Imprinted electrochemical sensor for dopamine recognition and determination based on a carbon nanotube/polypyrrole film. *Electrochimica Acta*, 2012. 63: p. 69-75.
- [12] Lu, X., et al., Polypyrrole/carbon nanotube nanocomposite enhanced the electrochemical capacitance of flexible graphene film for supercapacitors. *Journal of Power Sources*, 2012. 197: p. 319-324.
- [13] Lee, S.W., et al., Carbon Nanotube/Manganese Oxide Ultrathin Film Electrodes for Electrochemical Capacitors. *ACS nano*, 2010. 4(7): p. 3889-3896.
- [14] Toupin, M., T. Brousse, and D. Bélanger, Charge Storage Mechanism of MnO₂ Electrode Used in Aqueous Electrochemical Capacitor. *Chemistry of Materials*, 2004. 16(16): p. 3184-3190.
- [15] Rakhi, R.B., et al., Substrate Dependent Self-Organization of Mesoporous Cobalt Oxide Nanowires with Remarkable Pseudocapacitance. *Nano Letters*, 2012. 12(5): p. 2559-2567.
- [16] Zhang, F., et al., Flexible Films Derived from Electrospun Carbon Nanofibers Incorporated with Co₃O₄ Hollow Nanoparticles as Self-Supported Electrodes for Electrochemical Capacitors. *Advanced Functional Materials*, 2013. 23(31): p. 3909-3915.
- [17] Xu, W., B. Mu, et al. (2015). "Facile hydrothermal synthesis of tubular kapok fiber/MnO₂ composites and application in supercapacitors." *RSC Advances* 5(79): 64065-64075.
- [18] Sun, S., S. Wang, et al. (2015). "Hydrothermal synthesis of a MnOOH/three-dimensional reduced graphene oxide composite and its electrochemical properties for supercapacitors." *Journal of Materials Chemistry A* 3(42): 20944-20951.